Journal of Information Systems Engineering and Management
2021, 6(1)
e-ISSN: 2468-4376
https://www.jisem-journal.com/

Research Article

Taguchi-Based Regression Modelling and Optimisation of Surface Integrity Characteristics in Wire-Cut EDM of Titanium 6Al-4V ELI Alloy

Kanchan Rani [1*], V. K. Jha [2]
[1] Community College of Skill Development, J C Bose University of Science and Technology, YMCA, Faridabad, INDIA
[2] Department of Mechanical Engineering, Kalinga University, Raipur, INDIA
*Corresponding Author: kanch2202@gmail.com

ARTICLE INFO

Received: 11 Aug. 2020
Revised: 05 Oct. 2020
Accepted: 16 Jan. 2021

ABSTRACT

This paper reports a multi-response investigation and predictive modelling of the wire-cut electrical discharge machining (WEDM) of the biomedical titanium alloy Ti-6Al-4V ELI (Grade 23). Three surface-integrity responses, namely cutting rate, residual stress, and micro-hardness, were studied in relation to six controllable machining variables: flushing pressure, peak current, duty cycle, gap voltage, wire feed rate, and wire tension. A Taguchi L18 (2^1 × 3^5) orthogonal array was adopted as the design of experiments, and regression models relating the inputs to each response were developed in MINITAB-19. Analysis of variance (ANOVA) revealed that peak current, duty cycle, gap voltage and wire tension were the dominant factors, whereas flushing pressure and wire feed rate were comparatively insignificant. Both the cutting rate and the residual stress increased with rising peak current and duty cycle, while the mean micro-hardness of the machined surface was of the order of 208 HV. Higher flushing pressure and feed rate increased the cutting rate but reduced the residual stress (mean of about 212 MPa). The combined action of a high peak current and a high duty cycle was found to degrade the surface texture and to promote surface debris and micro-cracks, thereby elevating the residual stress. The study establishes a compact set of regression models and an optimal parameter window that can guide the WEDM of Ti-6Al-4V ELI for orthopaedic and aerospace applications.

Keywords: Wire-cut EDM, Titanium 6Al-4V ELI, Taguchi method, regression modelling, ANOVA, surface integrity, residual stress, micro-hardness.

Introduction

Over the past five decades, the development of orthopaedic implants has been shaped strongly by the introduction of new engineering materials such as titanium alloys, polyethylene and poly (methyl methacrylate), which are used for both temporary and permanent fixation (Planell & Navarro, 2009). Such implants can provide the short-term stabilisation of fractures, pseudarthroses and other bone defects, and can also permanently replace damaged sections of bone (Akono et al., 2012). Natural bone

is, in essence, a hierarchical composite of a fibrous polymer (collagen) and hard mineral nanoparticles (carbonated hydroxyapatite) that resists fracture across several length scales (Launey & Ritchie, 2009). Since titanium and its alloys were first used in the 1950s, this remarkable metal has steadily gained importance and has become a preferred choice for orthopaedic implants and for the aerospace industry.

Titanium alloys, and more specifically α+β alloys, have been widely investigated as candidate materials for orthopaedic and dental implants because of their attractive combination of properties. These include a high strength-to-weight ratio, good toughness, strong resistance to degradation under thermo-mechanical cycling, excellent surface stability in aggressive oxidising and corrosive environments, and good biocompatibility. The alloy offers high mechanical strength together with adequate ductility at a comparatively low density, and the vanadium content provides a high endurance limit, which is more significant for titanium implants than the ultimate strength alone (Ulutan & Ozel, 2011). The principal reason for selecting a titanium alloy for a clinical implant is its biocompatibility (Kaur & Singh, 2019). These properties also explain why Ti-6Al-4V is used in more than half of aerospace applications that employ titanium grades (Klocke et al., 2011).

Despite these advantages, several machining limitations associated with Ti-6Al-4V ELI mark it as a difficult-to-machine material, including its strong chemical reactivity over a wide temperature range and its low thermal conductivity. As a result, considerable research has focused on efficient methods for machining this alloy into complex shapes and profiles, generally through non-conventional machining processes (Danail et al., 2016). Among these, wire-cut electrical discharge machining (WEDM) has been studied extensively. The surface topography produced by WEDM is a composite property that reflects the deviation of the machined surface from the parent substrate; its constituent parameters include the residual stresses at the surface, the depth of the heat-affected layer and the micro-hardness, while geometrical and dimensional accuracy and surface roughness present further challenges (Che-Haron & Jawaid, 2005).

Micro-hardness plays a major role in describing the deviation of the machined surface from the substrate and may reasonably be used to characterise the surface topography of an EDM surface, since it is influenced by residual stresses, metallurgical changes and grain refinement (Kundrak et al., 2011). To sustain a high production rate together with an acceptable surface quality, it is therefore essential to select an appropriate combination of WEDM conditions — peak current, duty cycle, gap voltage and feed rate — because these variables govern multiple performance characteristics such as cutting rate, micro-hardness and residual stress, all of which are constituents of surface quality (Goel et al., 2012). The prevalence of micro-cracks in the recast layer can lower the measured micro-hardness, and the resulting mismatch between the surface and the bulk material can alter the mechanical properties and reduce the component's service life.

Among the many performance characteristics of WEDM, the cutting rate, residual stress and micro-hardness are particularly significant because they correlate directly with the surface profile (Oliver Nesa Raj and Prabhu, 2017). Machining costs and the residual stresses induced during WEDM are the chief concerns for the orthopaedic and aerospace industries today, as frictional forces gradually degrade the working surfaces of components and shorten their service life (Kumar et al., 2018; Ghanem et al., 2011). The surface morphology of implant and aerospace components is strongly affected by the residual stresses generated during machining (Rao et al., 2016): these stresses arise when regions of the material are non-homogeneously and plastically deformed, leaving strains of opposite sign within the surface layers. It is evident from the available literature that studies examining the influence of machining parameters on micro-hardness, a key surface-integrity parameter, have not yet been conducted exhaustively (Straka et al., 2016). With this in view, the present work selects these three surface characteristics for a multi-response study of the WEDM performance of Ti-6Al-4V ELI and develops regression models that relate them to the controllable process parameters.

Journal of Information Systems Engineering and Management
2021, 6(1)
e-ISSN: 2468-4376
https://www.jisem-journal.com/

Research Article

Experimental Details

A cylindrical bar of Ti-6Al-4V ELI (Grade 23) alloy, 10 mm in diameter and 50 cm long, was used for the experiments on a Sprintcut (Dlx) CNC wire-cut EDM machine. The chemical composition of the alloy was 6% Al, 4% V, 0.20% O, 0.015% P, 0.2% Fe, 0.06% C and the balance Ti. The material is suitable for a wide range of orthopaedic implants, aerospace components and automotive applications. Its mechanical properties include a Knoop hardness of 354 HRC, an ultimate tensile strength of 44 GPa, an elongation at break of 15%, a yield strength of 790 MPa and a shear modulus of 550 MPa. A preliminary trial was conducted to identify the machining variables that clearly influence WEDM performance; the six controllable factors and their levels are listed in Table 1.

Table 1. The controlled parameters and their levels of experimental design

Factor	Parameter	Level 1	Level 2	Level 3
A	Flushing Pressure	High (8)	Low (12)	-
B	Peak Current	90	120	150
C	Duty Cycle	60	65	70
D	Gap Voltage	20	30	40
E	Wire Feed Rate	3	7	11
F	Wire Tension	2	3	4

All remaining parameters were held constant. Since a positive electrode polarity is reported to provide a higher material removal rate, lower electrode wear, and a better surface finish (Niknam et al., 2014), a positive polarity was adopted, and de-ionised water served as the dielectric in all experiments.

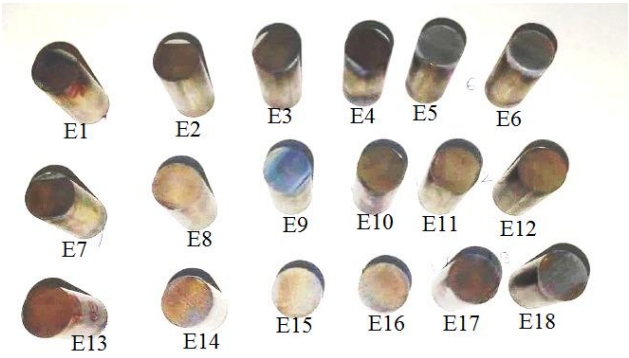

Figure 1. Titanium 6Al-4V ELI alloy — eighteen samples cut for experimentation

A Taguchi L18 (2^1 × 3^5) orthogonal array, comprising eight columns and eighteen rows, was used to organise the trials, of which two columns were treated as error. Each run was repeated three times, and the average value was recorded; the eighteen machined specimens prepared for the study are shown in Figure 1. The cutting rate (mm/min) was read directly from the machine display. Residual stress (MPa) was measured on the WEDM surface using a portable, non-destructive μ-X360 X-ray residual-stress analyser (Pulstec Industrial Corporation Ltd.), and the micro-hardness of the machined surface was determined with an AEC1107 auto-turret computerised micro-hardness tester (Ashian Engineering Company, India) under a 500 g load applied for a dwell time of 10 minutes.Within the Taguchi framework, the cutting rate is a higher-the-better characteristic and the residual stress is a lower-the-better characteristic. In this study, however, micro-hardness was treated as a nominal-the-better characteristic, because a slight increase in surface hardness after EDM has been found to be beneficial for the biomedical and orthodontic application of Ti-6Al-4V ELI (Wu et al., 2008). Using the Taguchi

Journal of Information Systems Engineering and Management
2021, 6(1)
e-ISSN: 2468-4376
https://www.jisem-journal.com/

Research Article

design together with analysis of variance (ANOVA), the optimal combination of WEDM parameters was then predicted for the alloy.

Results And Discussion

The experiments were designed using Taguchi's L18 (2^1 × 3^5) orthogonal array, and the measured response data are summarised in Table 2. The standard Taguchi procedure was followed for the analysis: the mean values and signal-to-noise (S/N) ratios of each response were examined at the different factor levels, and the main-effect trends for both the raw data and the S/N data were studied. The selection of regression models and the optimisation of responses were performed using the statistical package MINITAB-19.

Table 2. Experimental results for cutting rate, residual stress and micro-hardness

Ex. No.	Machining parameters						Cutting rate (mm/min)				Residual stress (MPa)				Micro-hardness (HV)			
	A	B	C	D	E	F	R1	R2	R3	S/N	R1	R2	R3	S/N	R1	R2	R3	S/N
1	8	120	60	20	3	7	0.40	0.36	0.42	-8.16	103	109	98	-40.29	174	178	169	-13.08
2	8	120	65	30	4	11	1.73	1.72	1.79	4.84	235	211	256	-47.41	239	241	238	-3.68
3	8	120	70	40	2	3	1.66	1.78	1.55	4.38	156	145	166	-43.86	193	189	197	-12.04
4	8	150	60	30	2	11	1.33	1.36	1.11	1.94	181	198	165	-45.19	191	188	195	-10.91
5	8	150	65	40	3	3	2.04	2.19	1.80	5.98	241	221	256	-47.60	222	214	231	-18.59
6	8	150	70	20	4	7	1.80	1.82	1.78	5.10	261	248	276	-48.36	241	245	236	-13.08
7	12	90	60	40	4	7	1.90	1.80	1.95	5.48	244	238	249	-47.74	238	241	238	-4.77
8	12	90	65	20	2	11	2.24	2.21	2.23	6.95	306	312	294	-49.66	258	256	259	-3.68
9	12	90	70	30	3	3	2.23	2.16	2.33	6.99	241	245	237	-47.64	221	226	221	-9.21
10	12	120	60	30	4	3	0.98	1.01	1.09	0.20	54	66	44	-34.87	149	142	141	-12.79
11	12	120	65	40	2	7	0.85	0.75	0.80	-1.97	119	125	110	-41.45	147	142	151	-13.08
12	12	120	70	20	3	11	2.17	2.12	2.22	6.72	282	295	274	-49.06	238	228	247	-19.56
13	12	150	60	40	3	11	1.73	1.75	1.72	4.78	199	188	212	-46.02	201	206	195	-14.82
14	12	150	65	20	4	3	1.50	1.51	1.48	3.50	188	201	178	-45.54	194	197	196	-3.68
15	12	150	70	30	2	7	2.15	2.16	2.01	6.46	257	266	251	-48.23	187	188	184	-6.37

Journal of Information Systems Engineering and Management
2021, 6(1)
e-ISSN: 2468-4376
https://www.jisem-journal.com/

Research Article

Ex. No.	Machining parameters						Cutting rate (mm/min)				Residual stress (MPa)				Micro-hardness (HV)			
	A	B	C	D	E	F	R1	R2	R3	S/N	R1	R2	R3	S/N	R1	R2	R3	S/N
16	8	120	60	20	3	7	2.09	1.90	2.11	6.13	218	221	210	-46.70	197	189	206	-18.59
17	8	120	65	30	4	11	1.87	1.95	1.75	5.35	222	226	216	-46.90	192	188	197	-13.08
18	8	120	70	40	2	3	2.62	2.69	2.59	8.41	312	325	304	-49.93	256	252	259	-10.91

A = Flushing pressure; B = Peak current; C = Duty cycle; D = Gap voltage; E = Wire feed rate; F = Wire tension. R1–R3 are repetitions; S/N is the signal-to-noise ratio (dB): larger-the-better for cutting rate, smaller-the-better for residual stress, nominal-the-better for micro-hardness.

Effect of process variables on cutting rate

The estimated regression coefficients for the mean cutting rate, listed in Table 3, were obtained from the experimental data of Table 2. The model expresses the cutting rate as a function of the six input variables, including the interaction between flushing pressure and peak current. As the coefficient of this interaction is very small (0.00259) and was found to be insignificant by ANOVA, it may be omitted from the model without appreciable loss of accuracy.

Table 3. Estimated model coefficients for the mean cutting rate

Term	Level	Coefficient	SE Coef.	T	P-Value
Constant		1.72704	0.004061	425.229	0.000
Flushing Pressure	8	-0.03481	0.004061	-8.572	0.001
Peak Current	90	-0.42704	0.005744	-74.348	0.000
Peak Current	120	0.00852	0.005744	1.483	0.212
Duty Cycle	60	-0.33759	0.005744	-58.776	0.000
Duty Cycle	65	-0.03759	0.005744	-6.545	0.003
Gap Voltage	20	-0.28315	0.005744	-49.297	0.000
Gap Voltage	30	0.30241	0.005744	52.650	0.000
Wire Tension	2	-0.22593	0.005744	-39.334	0.000
Wire Tension	3	0.19796	0.005744	34.466	0.000
Wire Feed Rate	3	-0.03037	0.005744	-5.288	0.006
Wire Feed Rate	7	0.00796	0.005744	1.386	0.238
Flushing*Peak Current	8, 90	0.00259	0.005744	0.451	0.675
Flushing*Peak Current	8, 120	-0.00852	0.005744	-1.483	0.212

The ANOVA results for the cutting rate, given in Tables 4 and 5 for the S/N and mean data, respectively, quantify the relative contribution of each machining variable. They show that wire feed rate and flushing pressure are the least significant factors, while peak current, duty cycle, gap voltage and wire tension contribute significantly to the cutting rate of the Ti-6Al-4V ELI alloy.

Journal of Information Systems Engineering and Management
2021, 6(1)
e-ISSN: 2468-4376
https://www.jisem-journal.com/

Research Article

Table 4. ANOVA for the cutting rate (S/N ratio data)

Source	DF	Seq SS	Adj SS	Adj MS	F	P
Flushing Pressure	1	2.045	2.045	2.0453	0.95	0.384
Peak Current	2	95.321	95.321	47.6604	22.20	0.007
Duty Cycle	2	63.874	63.874	31.9370	14.88	0.014
Gap Voltage	2	55.521	55.521	27.7603	12.93	0.018
Wire Tension	2	38.407	38.407	19.2037	8.95	0.033
Wire Feed Rate	2	3.298	3.298	1.6490	0.77	0.522
Flushing*Peak Current	2	1.007	1.007	0.5037	0.23	0.801
Residual Error	4	8.586	8.586	2.1466		
Total	17	268.060				

Table 5. ANOVA for the cutting rate (mean data)

Source	DF	Seq SS	Adj SS	Adj MS	F	P
Flushing Pressure	1	0.02182	0.02182	0.02182	73.48	0.001
Peak Current	2	2.14555	2.14555	1.07277	3613.08	0.000
Duty Cycle	2	1.53688	1.53688	0.76844	2588.09	0.000
Gap Voltage	2	1.03196	1.03196	0.51598	1737.82	0.000
Wire Tension	2	0.54608	0.54608	0.27304	919.60	0.000
Wire Feed Rate	2	0.00893	0.00893	0.00446	15.03	0.014
Flushing*Peak Current	2	0.00069	0.00069	0.00034	1.16	0.402
Residual Error	4	0.00119	0.00119	0.00030		
Total	17	5.29309				

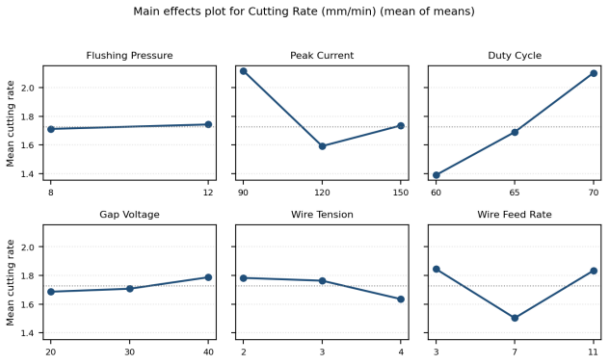

Figure 2. Main-effects plot for the mean cutting rate

Figure 2 presents the main-effects plot for the mean cutting rate. The cutting rate rises with increasing flushing pressure, peak current, duty cycle and wire feed rate. A higher flushing pressure improves dielectric exchange within the gap and helps flush debris, while a higher peak current and duty cycle deliver greater discharge energy. However, very high values of peak current, duty cycle, and wire feed rate increase the risk of wire breakage and wire deflection, which limit the efficiency and accuracy of the process and can reduce the effective machining speed, adversely affecting the overall productivity of the operation. The cutting rate is thus proportional to the energy consumed during machining, depending not only on the energy per pulse, which determines the crater size, but also on

Journal of Information Systems Engineering and Management
2021, 6(1)
e-ISSN: 2468-4376
https://www.jisem-journal.com/

Research Article

the applied power. As the duty cycle increases, the mean discharge gap widens, which can, in turn, reduce the cutting rate.

Effect of process variables on residual stress

The high temperature gradient developed during a discharge is sufficient to melt and partly vaporise the work material, which then re-solidifies on the machined surface. This not only produces an inconsistent and degraded surface but also induces residual stress, the magnitude of which can exceed the parent material's yield point, thereby altering the local yield strength of the machined surface. The estimated regression coefficients for the mean residual stress are given in Table 6. As before, the model includes the flushing pressure–peak current interaction, whose coefficient (0.019) is statistically insignificant and may be neglected.

Table 6. Estimated model coefficients for the mean residual stress

Term	Level	Coefficient	SE Coef.	T	P-Value
Constant		212.130	0.1410	1504.115	0.000
Flushing Pressure	8	6.093	0.1410	43.200	0.000
Peak Current	90	-53.907	0.1995	-270.280	0.000
Peak Current	120	9.370	0.1995	46.981	0.000
Duty Cycle	60	-45.630	0.1995	-228.777	0.000
Duty Cycle	65	5.481	0.1995	27.483	0.000
Gap Voltage	20	-24.963	0.1995	-125.159	0.000
Gap Voltage	30	40.204	0.1995	201.572	0.000
Wire Tension	2	-7.241	0.1995	-36.303	0.000
Wire Tension	3	34.093	0.1995	170.933	0.000
Wire Feed Rate	3	16.815	0.1995	84.306	0.000
Wire Feed Rate	7	-9.852	0.1995	-49.395	0.000
Flushing*Peak Current	8, 90	0.019	0.1995	0.093	0.930
Flushing*Peak Current	8, 120	-0.148	0.1995	-0.743	0.499

The ANOVA for the residual stress is summarised in Tables 7 and 8. The analysis (lower-the-better) confirms that wire feed rate and flushing pressure are insignificant, whereas peak current, duty cycle, gap voltage and wire tension are the significant contributors to the surface residual stress. The residual stress is observed to increase in proportion to the cutting rate.

Table 7. ANOVA for the residual stress (S/N ratio data)

Source	DF	Seq SS	Adj SS	Adj MS	F	P
Flushing Pressure	1	4.541	4.541	4.541	2.57	0.184
Peak Current	2	90.850	90.850	45.425	25.74	0.005
Duty Cycle	2	59.884	59.884	29.942	16.97	0.011
Gap Voltage	2	37.655	37.655	18.828	10.67	0.025
Wire Tension	2	32.481	32.481	16.240	9.20	0.032
Wire Feed Rate	2	7.854	7.854	3.927	2.23	0.224
Flushing*Peak Current	2	2.510	2.510	1.255	0.71	0.544
Residual Error	4	7.059	7.059	1.765		

Journal of Information Systems Engineering and Management
2021, 6(1)
e-ISSN: 2468-4376
https://www.jisem-journal.com/

Research Article

Source	DF	Seq SS	Adj SS	Adj MS	F	P
Total	17	242.834				

Table 8. ANOVA for the residual stress (mean data)

Source	DF	Seq SS	Adj SS	Adj MS	F	P
Flushing Pressure	1	668.2	668.2	668.2	1866.22	0.000
Peak Current	2	29864.2	29864.2	14932.1	41706.84	0.000
Duty Cycle	2	22343.9	22343.9	11172.0	31204.41	0.000
Gap Voltage	2	14830.6	14830.6	7415.3	20711.71	0.000
Wire Tension	2	11614.5	11614.5	5807.3	16220.29	0.000
Wire Feed Rate	2	2569.7	2569.7	1284.8	3588.69	0.000
Flushing*Peak Current	2	0.2	0.2	0.1	0.33	0.738
Residual Error	4	1.4	1.4	0.4		
Total	17	81892.7				

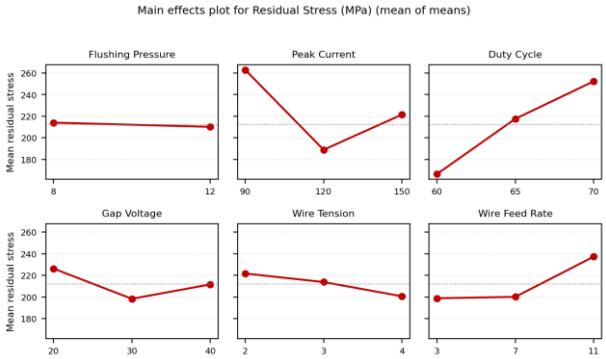

Figure 3. Main-effects plot for the mean residual stress

As shown in Figure 3, the residual stress of the machined surface increases with peak current and duty cycle. The discharge energy within the gap is a function of the pulse peak current and the pulse-on time; a higher peak current and duty cycle prolong the pulse-on time and increase the discharge energy, which in turn raises the residual stress. The sensitivity of the residual stress to peak current is, however, stronger than its sensitivity to duty cycle. The middle range of gap voltage and feed rate also leads to high residual stress, whereas increasing the flushing pressure and wire tension has comparatively little effect.

Effect of process variables on micro-hardness

The estimated regression coefficients for the mean micro-hardness are presented in Table 9, again derived from the data of Table 2 under the nominal-the-better criterion. The coefficients of the flushing pressure–peak current interaction (0.537) and of wire tension (0.556) are insignificant according to ANOVA and may be omitted from the model.

Table 9. Estimated model coefficients for the mean micro-hardness

Term	Level	Coefficient	SE Coef.	T	P-Value
Constant		488.556	0.4279	1141.661	0.000
Flushing Pressure	8	12.407	0.4279	28.994	0.000
Peak Current	90	-18.500	0.6052	-30.569	0.000

Journal of Information Systems Engineering and Management
2021, 6(1)
e-ISSN: 2468-4376
https://www.jisem-journal.com/

Research Article

Term	Level	Coefficient	SE Coef.	T	P-Value
Peak Current	120	-1.389	0.6052	-2.295	0.083
Duty Cycle	60	-16.556	0.6052	-27.356	0.000
Duty Cycle	65	1.444	0.6052	2.387	0.075
Gap Voltage	20	-22.056	0.6052	-36.444	0.000
Gap Voltage	30	24.889	0.6052	41.126	0.000
Wire Tension	2	1.000	0.6052	1.652	0.174
Wire Tension	3	10.722	0.6052	17.717	0.000
Wire Feed Rate	3	9.556	0.6052	15.789	0.000
Wire Feed Rate	7	0.556	0.6052	0.918	0.411
Flushing*Peak Current	8, 90	0.537	0.6052	0.887	0.425
Flushing*Peak Current	8, 120	-0.463	0.6052	-0.765	0.487

The corresponding ANOVA results for the micro-hardness are given in Tables 10 and 11. As illustrated in Figure 4, the micro-hardness increases with peak current and duty cycle, while a decreasing trend is observed with wire feed rate; the effects of gap voltage, feed rate and wire tension are comparatively uncertain. Peak current emerges as the most dominant parameter governing the surface micro-hardness, and the WEDM parameters can therefore be selected so as to enhance the surface micro-hardness of the Ti-6Al-4V ELI alloy.

Table 10. ANOVA for the micro-hardness (S/N ratio data)

Source	DF	Seq SS	Adj SS	Adj MS	F	P
Flushing Pressure	1	18.42	18.42	18.419	0.66	0.464
Peak Current	2	18.52	18.52	9.259	0.33	0.737
Duty Cycle	2	30.96	30.96	15.479	0.55	0.615
Gap Voltage	2	18.46	18.46	9.229	0.33	0.738
Wire Feed Rate	2	24.94	24.94	12.472	0.44	0.670
Wire Tension	2	37.62	37.62	18.809	0.67	0.562
Flushing*Peak Current	2	77.09	77.09	38.543	1.37	0.352
Residual Error	4	112.46	112.46	28.114		
Total	17	338.46				

Table 11. ANOVA for the micro-hardness (mean data)

Source	DF	Seq SS	Adj SS	Adj MS	F	P
Flushing Pressure	1	2771.0	2770.99	2770.99	840.64	0.000
Peak Current	2	4438.5	4438.48	2219.24	673.25	0.000
Duty Cycle	2	3027.1	3027.11	1513.56	459.17	0.000
Gap Voltage	2	6683.6	6683.59	3341.80	1013.80	0.000
Wire Feed Rate	2	1520.3	1520.26	760.13	230.60	0.000
Wire Tension	2	1163.1	1163.11	581.56	176.43	0.000
Flushing*Peak Current	2	3.0	3.05	1.52	0.46	0.660
Residual Error	4	13.2	13.19	3.30		
Total	17	19619.8				

Journal of Information Systems Engineering and Management
2021, 6(1)
e-ISSN: 2468-4376
https://www.jisem-journal.com/

Research Article

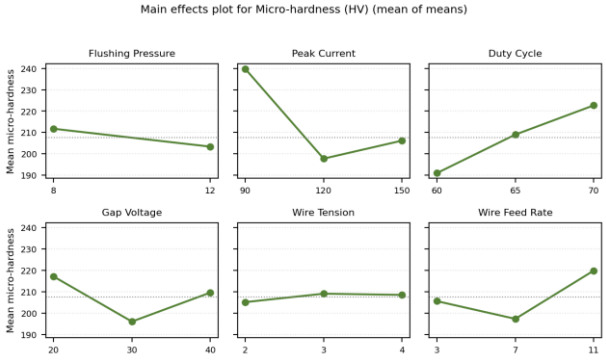

Figure 4. Main-effects plot for the mean micro-hardness

The elevated micro-hardness is associated with the amount of debris remaining on the alloy's machined surface; such surface irregularities are, in fact, desirable on an implant surface because they encourage cell growth around the implant (Jahan et al., 2017). While investigating the influence of surface micro-hardness on biocompatibility, it was confirmed that a modest increase in hardness after WEDM can be beneficial for the biomedical and orthodontic application of Ti-6Al-4V ELI (Wu et al., 2008). The residual analysis, used as a diagnostic tool, indicated that the data points follow the fitted straight line closely and are therefore normally distributed, which confirms that the assumptions underlying the regression models are valid.

Prediction of the optimum process parameters

Table 12 lists the factor levels that yield the highest and lowest predicted values of each response. For the cutting rate, the highest predicted level combination is A2 B3 C2 D3 E2 F3 and the lowest is A1 B1 C1 D1 E1 F2. For the residual stress, the highest predicted combination is A1 B3 C3 D2 E2 F1 and the lowest is A2 B1 C1 D1 E3 F2. For the micro-hardness, the highest predicted combination is A2 B3 C2 D3 E1 F2, while the optimum (minimum) combination is A1 B1 C1 D1 E1 F1.

Table 12. Predicted optimum levels of the input variables

Parameter	Cutting rate – Lowest	Cutting rate – Highest	Residual stress – Lowest	Residual stress – Highest	Micro-hardness – Lowest	Micro-hardness – Highest
Flushing Pressure	8	12	12	8	8	12
Peak Current	90	150	90	150	90	150
Duty Cycle	60	65	60	75	60	65
Gap Voltage	20	40	20	30	20	40
Wire Tension	2	7	11	7	3	3
Wire Feed Rate	3	4	3	2	2	3
Predicted Mean	0.388	2.159	44.833	394.019	454.944	539.667

Conclusion

This paper reports the application of the Taguchi method, supported by regression modelling, to improve multiple performance characteristics — cutting rate, residual stress, and micro-hardness — in wire-cut EDM of Ti-6Al-4V ELI (Grade 23) alloy. The Taguchi design of experiments greatly simplified the optimisation of these coupled characteristics, and the regression models developed in MINITAB-19 captured the relationship between the six process variables and each response with a high degree of statistical significance.

The ANOVA showed that peak current, duty cycle, gap voltage and wire tension were the dominant factors, while flushing pressure and wire feed rate were comparatively insignificant. The machining performance, expressed as cutting rate, was directly proportional to the peak current and duty cycle, and the residual stress followed the same trend. The selected WEDM conditions also enhanced the alloy's surface micro-hardness, which is favourable for its biomedical application.

On the basis of the experimental data, the optimal process parameters for the WEDM of Ti-6Al-4V ELI comprised a flushing pressure of 8 units, a peak current of 90 A, a duty cycle of 60% and a gap voltage of 20 V. For the predicted optimum residual stress, the settings were a flushing pressure of 8 units (level 1), a peak current of 90 A (level 1), a duty cycle of 60% (level 1), a gap voltage of 20 V (level 1), a wire feed rate of 3 mm/min (level 1) and a wire tension of level 1. For the optimum micro-hardness, the same flushing pressure, peak current, duty cycle and gap voltage are applied, with a wire feed rate of 3 mm/min (level 1) and a wire tension of level 2. For the optimum cutting rate, the corresponding settings were a flushing pressure of 8 units, a peak current of 90 A, a duty cycle of 60%, a gap voltage of 20 V, a wire feed rate of 3 mm/min and a wire tension of level 2. These results provide a practical parameter window for machining the alloy, and further work on a wider parameter range is recommended to explore its influence on the fatigue life and wear resistance of the proposed alloy.

Author contributions: Both authors contributed to all stages of this study and approved the final version of the manuscript.

Funding: No external funding was received for this article.

Declaration of interest: The authors declare no competing interests.

References

[1] Akono, A. T., Randall, N. X. and Ulm, F. J. (2012). Experimental determination of the fracture toughness via microscratch tests: Application to polymers, ceramics, and metals. Journal of Materials Research, 27(2), 485-493. https://doi.org/10.1557/jmr.2011.402

[2] Che-Haron, C. H. and Jawaid, A. (2005). The effect of machining on surface integrity of titanium alloy Ti-6Al-4V. Journal of Materials Processing Technology, 166(2), 188-192. https://doi.org/10.1016/j.jmatprotec.2004.08.012

[3] Danail, G., Nikolay, F. and Stoyan, D. (2016). Classification, properties and application of titanium and its alloys. Proceedings of the University of Ruse, 55, 27-32.

[4] Ghanem, F., Ben Fredj, N., Sidhom, H. and Braham, C. (2011). Effects of finishing processes on the fatigue life improvements of electro-machined surfaces of tool steel. International Journal of Advanced Manufacturing Technology, 52, 583-595. https://doi.org/10.1007/s00170-010-2751-y

[5] Goel, P., Khan, Z. A., Siddiquee, A. N., Kamaruddin, S. and Gupta, R. K. (2012). Influence of slab milling process parameters on surface integrity of HSLA: A multi-performance characteristics optimization. International Journal of Advanced Manufacturing Technology, 61, 859-871.

[6] Jahan, M. P., Kakavand, P. and Alavi, F. (2017). A comparative study on micro-electro-discharge-machined surface characteristics of Ni-Ti and Ti-6Al-4V with respect to biocompatibility. Procedia Manufacturing, 10, 232-242. https://doi.org/10.1016/j.promfg.2017.07.051

[7] Kaur, M. and Singh, K. (2019). Review on titanium and titanium based alloys as biomaterials for orthopaedic applications. Materials Science and Engineering: C, 102, 844-862. https://doi.org/10.1016/j.msec.2019.04.064

[8] Klocke, F., Welling, D. and Dieckmann, J. (2011). Comparison of grinding and wire EDM concerning fatigue strength and surface integrity of machined Ti-6Al-4V components. Procedia Engineering, 19, 184-189. https://doi.org/10.1016/j.proeng.2011.11.099

[9] Kumar, S., Grover, S. and Walia, R. S. (2018). Effect of hybrid wire EDM conditions on generation of residual stresses in machining of HCHCr D2 tool steel under ultrasonic vibration. International Journal on Interactive Design and Manufacturing, 12, 1119-1137. https://doi.org/10.1007/s12008-018-0474-8

[10] Kundrak, J., Mamalis, A. G., Gyani, K. and Bana, V. (2011). Surface layer microhardness changes with high-speed turning of hardened steels. International Journal of Advanced Manufacturing Technology, 53, 105-112. https://doi.org/10.1007/s00170-010-2840-y

[11] Launey, M. E. and Ritchie, R. O. (2009). On the fracture toughness of advanced materials. Advanced Materials, 21(20), 2103-2110. https://doi.org/10.1002/adma.200803322

[12] Niknam, S. A., Khettabi, R. and Songmene, V. (2014). Machinability and machining of titanium alloys: A review, in J. P. Davim (ed.), Machining of Titanium Alloys. Berlin: Springer. https://doi.org/10.1007/978-3-662-43902-9_7

[13] Oliver Nesa Raj, S. and Prabhu, S. (2017). Modeling and analysis of titanium alloy in wire-cut EDM using grey relation coupled with principal component analysis. Australian Journal of Mechanical Engineering, 15(3), 198-209. https://doi.org/10.1080/14484846.2016.1251077

[14] Planell, J. A. and Navarro, M. (2009). Challenges of bone repair, in Bone Repair Biomaterials. Amsterdam: Elsevier, pp. 3-24.

[15] Rao, P. S., Ramji, K. and Satyanarayana, B. (2016). Effect of wire EDM conditions on generation of residual stresses in machining of aluminum 2014 T6 alloy. Alexandria Engineering Journal, 55(2), 1077-1084.

[16] Straka, L., Čorný, I. and Pitel, J. (2016). Properties evaluation of thin microhardened surface layer of tool steel after wire EDM. Metals, 6(5), 95. https://doi.org/10.3390/met6050095

[17] Ulutan, D. and Ozel, T. (2011). Machining induced surface integrity in titanium and nickel alloys: A review. International Journal of Machine Tools and Manufacture, 51(3), 250-280. https://doi.org/10.1016/j.ijmachtools.2010.11.003

[18] Wu, C., Ramaswamy, Y., Gale, D., Yang, W., Xiao, K., Zhang, L., Yin, Y. and Zreiqat, H. (2008). Novel sphene coatings on Ti-6Al-4V for orthopedic implants using sol-gel method. Acta Biomaterialia, 4(3), 569-576. https://doi.org/10.1016/j.actbio.2007.11.005